

Dynamic Monitoring of Tannin-based Foam Preparation: Effects of Surfactant

Maria Cecilia Basso,^{a,b} Antonio Pizzi,^{a,c,*} and Alain Celzard^d

Three tannin-based foam formulations differing in the type of surfactant added were tested during foaming *via* simultaneous monitoring of the variation in temperature, foam rising rate, internal foam pressure, and dielectric polarization, the latter being a direct measure of the setting and curing of a thermosetting foam. This monitoring is an effective descriptor of the process and possible characteristics of the foam being prepared and constitutes an invaluable tool for foam formulation. The addition of a surfactant was shown to have a major effect on foam dynamics by retarding the onset of cross-linking to a lesser or greater extent in relation to the peak of maximum temperature in self-blowing foams. Cationic surfactants, or non-ionic surfactants capable of transforming into cationic species under the acidic environmental conditions used for tannin-based foams, were found to retard cross-linking more markedly than did non-ionic surfactants.

Keywords: Tannin foams; Surfactant effect; Foaming temperature; Dielectric polarization; Foaming pressure; Foam rising rate; Foam curing; Simultaneous measure

Contact information: a: LERMAB, Universite de Lorraine, 27 Rue Philippe Seguin, 88000 Epinal, France; b: SILVA-INDUNOR, Cerrito 1136 (C 1010AAX), Buenos Aires, Argentina; c: King Abdulaziz University, Jeddah, Saudi Arabia; d: IJL, Universite de Lorraine, 27 Rue Philippe Seguin, 88000 Epinal, France; *Corresponding author: antonio.pizzi@univ-lorraine.fr

INTRODUCTION

Polyflavonoid tannin-furanic rigid foams have been developed and tested for a number of different applications (Basso *et al.* 2013a; Tondi *et al.* 2008, 2009a). These foams are biosourced materials that perform well in a number of different capacities (Meikleham and Pizzi 1994; Pizzi *et al.* 2008; Tondi *et al.* 2009b; Li *et al.* 2012a,b,c, 2013; Lacoste *et al.* 2013a,b). The formulation of the combination of materials appropriate for achieving the properties desired for a particular application is a difficult undertaking. This is because the self-blowing mixture of resins and additives needs to be well balanced with respect to its simultaneous foaming and setting. That is, the characteristics of early foaming and late setting, and likewise of early setting and late foaming, will not produce a rigid hardened foam (Tondi and Pizzi 2009).

Recently, a method and corresponding equipment capable of dynamically monitoring the main parameters from which the preparation of any foam depends has been used to study the process of foaming leading to tannin-based rigid foams (Basso *et al.* 2013b). These parameters are (i) the rise and fall of the temperature generated by the reaction from which foaming depends; (ii) the setting and curing rate of the polymers or copolymers that are the main constituents of the foam, which is measured by means of dielectric polarization (dielectric polarization is a well-known technique used in other fields to monitor the setting and curing of a thermoset resin (Sernek and Kamke 2007) by measuring the decrease in molecular mobility during cross-linking); (iii) the velocity at

which the mixture rises during foaming; and (iv) the internal pressure that develops inside the mixture during foaming. It is the combination and monitoring of these parameters “*in situ*” that allows the rapid determination of which type of foam is being prepared.

This paper describes how this method can be finely tuned by studying small variations in the surfactants during the foaming and curing process of tannin-based foams.

EXPERIMENTAL

Tannin

Commercial tannin powder, sold under the name Fintan OP and supplied by the company SilvaChimica (St. Michele Mondovi, Italy), was used. The tannin was extracted industrially in Tanzania from the whole dried bark of 10-year-old mimosa trees (*Acacia mearnsii*, formerly *mollissima*, de Wild). Tannin consists of more than 80% phenolic (flavonoid) materials, the remainder being water, amino and imino acid fractions, hydrocolloid gums, and carbohydrates, which are in general broken pieces of hemicelluloses (Pizzi 1983). In mimosa tannin, prorobinetinidin represents about 70% of the phenolic component, *i.e.*, the main flavonoid unit (Fig. 1). Such units are mostly 4,6-linked, and sometimes 4,8-linked, leading to oligomers whose molecular weights typically range from 500 to 3500 g mol⁻¹. More details regarding the degree of polymerization of the oligomers have been given in previous studies (Pizzi 1983; Pasch *et al.* 2001).

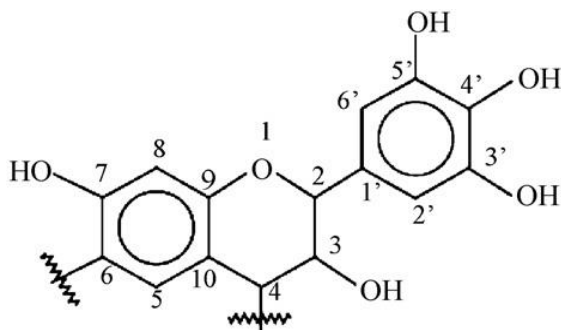


Fig. 1. Prorobinetinidin, the main flavonoid unit contained in wattle tannin

The analysis of commercial extract of mimosa shows 6 to 7% moisture content, insolubles content of 1%, pH (1% sol.) of 4.5 to 5.3, ash content of 3% (max.), and acids content (as meq H⁺) of 16.9.

Preparation of Foams

The method used to prepare the rigid tannin-based foams has been described in previous studies (Meikleham and Pizzi 1994; Tondi and Pizzi 2009; Celzard *et al.* 2011). In short, the mimosa bark tannin extracts (Silva Chimica, St. Michele Mondovi, Italy) were mixed with water, furfuryl alcohol was added as a co-reagent, formaldehyde was added as a further cross-linker, and diethyl ether was added as a blowing agent. The other

additives, as indicated in Table 1, were premixed with the furfuryl alcohol, and the mixture was mechanically stirred until it had become a homogeneous viscous liquid. Finally, a solution of 65% p-toluensulphonic acid (pTSA) was added as a catalyst. The exothermic energy released by the self-polymerization of the furfuryl alcohol and its reaction with the tannin led to the boiling of the blowing agent and the consequent, almost simultaneous, foaming and setting of the mixture. After foaming, the samples were left to age for a few days and then were cut into specimens.

Table 1. Foam Formulations (in Grams) used for Dynamic Testing during Foaming

Formulation	MN8'	MN21	MN18
Mimosa Tannin Extract	30	30	30
pTSA 65%	11	11	11
Formaldehyde 37%	7.4	7.4	7.4
Furfuryl Alcohol	10.5	10.5	10.5
Water	6	6	6
Diethyl ether	3	3	3
Ethoxylated Castor Oil 35 mol	0.6		
PEG400	8	8	8
Pluronic PE 6400		0.6	
Ethoxylated fatty amine 12 moles			0.6
Density (g/cm ³) ± 0,005	0.055	0.058	0.078

The foams shown in Table 1 correspond to formulations with three different non-ionic surfactants/dispersing agents (Tadros 2005). These are (i) Pluronic PE 6400 (ethylene glycol propylene glycol copolymer) with the formula HO-(CH₂-CH₂-O)_N-(CH₂-CH(CH₃)-O)_M-(CH₂-CH₂)-OH for MN21, (ii) PEG35 castor oil (that is, polyoxyl hydrogenated castor oil, an ethoxylated castor oil) for MN8', and (iii) an ethoxylated fatty amine (coconut amine ethoxylate) such as H-(O-CH₂-CH₂)_X-N(R)-(CH₂-CH₂-O)_Y-H for MN18, the latter of which transforms into a cationic surfactant at certain acid pHs (Tadros 2005). All were of the same proportion for the three foam formulations.

Foams Characterization

All the foams were cut into parallelepipeds and weighed in order to measure their bulk density. All were homogeneous and flawless.

Tomography studies were carried out. Standard scaffold analysis was applied and the following scaffold modules were used: SCAF, R10, Version V1.0. The scaffolds were scanned by microcomputed tomography (microCT) using the following parameters: Energy 45 kVp; Intensity 88 mA; Integration time 200 ms; Frame averaging 2×; Nominal resolution 7.4 mm (isotropic). For image processing the measured data was filtered using a constrained Gaussian filter with finite filter support (1 voxel) and filter width (= 0.8). The images were then binarized to separate the object from the background using a global thresholding procedure. A component labeling algorithm was subsequently applied to remove all unconnected parts which typically arise from image noise. These final images were then analyzed with standard morphometric algorithms (Hildebrand and Ruesegger, 1996; Odgaard, 1997; Odgaard and Gundersen, 1993). A centered volume of interest (VOI) was digitally extracted from the measured data. The VOI was selected to be a cuboid of 5 × 5 × 4.5 mm³ edge length (i.e. 672 × 672 × 606 voxels). Selecting a digital

subvolume reduces boundary artifacts that may occur from simple preparation. A threedimensional representation of each scaffold was created.

Characterization of the Foaming Process

The curves describing the expansion, hardening, and temperature and pressure variation as a function of time for the three foam formulations were determined simultaneously using a FOAMAT apparatus, Model 281 (Foamat Messtechnik GmbH, Karlsruhe, Germany). This device comprises:

- ultrasonic sensor which measured the height of the foam.
- thermocouple K-type to record the temperature.
- CMD 2 (Curing Monitor Device) – sensor allowing the measurement of the electrochemical properties of foam during the transition from fluid to solid (Dielectric polarization).
- FPM 2 (Foams Pressure Measurement)-sensor, 100 mm diameter, allowing the measurement of the pressure.

The different measuring sensors were controlled using the program MOUSSE, version 3.8. For each incidence of foaming following the mixture preparation, the mixture was quickly poured into a suitable foaming chamber, namely a carton cylinder, supplied with the measuring equipment which was previously placed upon the manometer. The force applied to this metal plate sensor was used as a measure of the pressure generated by the expansion of the material upon foaming. The temperature was measured simultaneously using the thermocouple immersed within the mixture. The setting/curing/hardening rate profile of the foams was measured simultaneously by means of the dielectric polarization sensor composed of two comb-shaped electrodes arranged on a printed circuit in such a manner as to form a type of flat condenser. This sensor was integrated into the pressure-measuring device located at the bottom of the foaming chamber, *i.e.* the carton cylinder. The blowing pressure ensured contact between the foaming sample and the polarization sensor and consequently ensured the direct penetration of the electrical field.

The foam height during its expansion was constantly monitored by the ultrasound sensor placed over the foaming chamber. This device functions according to the “pulse-echo” method, meaning that foam height, and thus rising rate, is determined instantaneously based on the time required for the acoustic pulse to strike the surface of the expanding foam and to return to the sensor. The ultrasonic sensor is a membrane-type converter used as both an acoustic transmitter and receptor.

The foaming experiment was done three times for each formulation in order to confirm the measured trends.

RESULTS AND DISCUSSION

The variation in the four parameters as a function of time is shown in Figs. 2-5 and 6. In Fig. 2, the curves representing variation in temperature show that while the rate at which temperature increased was similar for the three formulations, the peak temperature was slightly higher for the MN8' foam in relation to the other two, and there was a slight difference in the time at which the maximum temperature was reached (200 s for the MN8', 230 s for the MN21, and 280 s for the MN18). The three formulations showed the same trend with respect to the decrease in temperature, although the rate of

cooling was the inverse of the rate of heating, with MN18 cooling slower than MN21 or MN8'. From the appearance of Fig. 2, it appears that the differences in temperature variation between the different formulations are not significant.

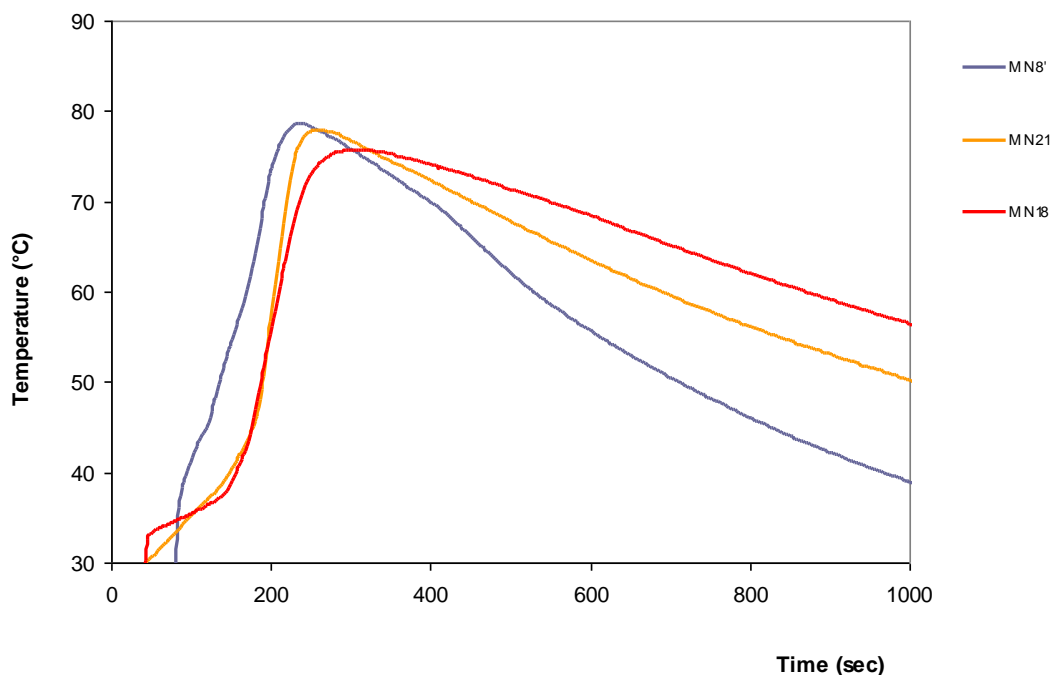


Fig. 2. Curves of temperature variation as a function of time during foaming for the MN8', MN21, and MN18 foams

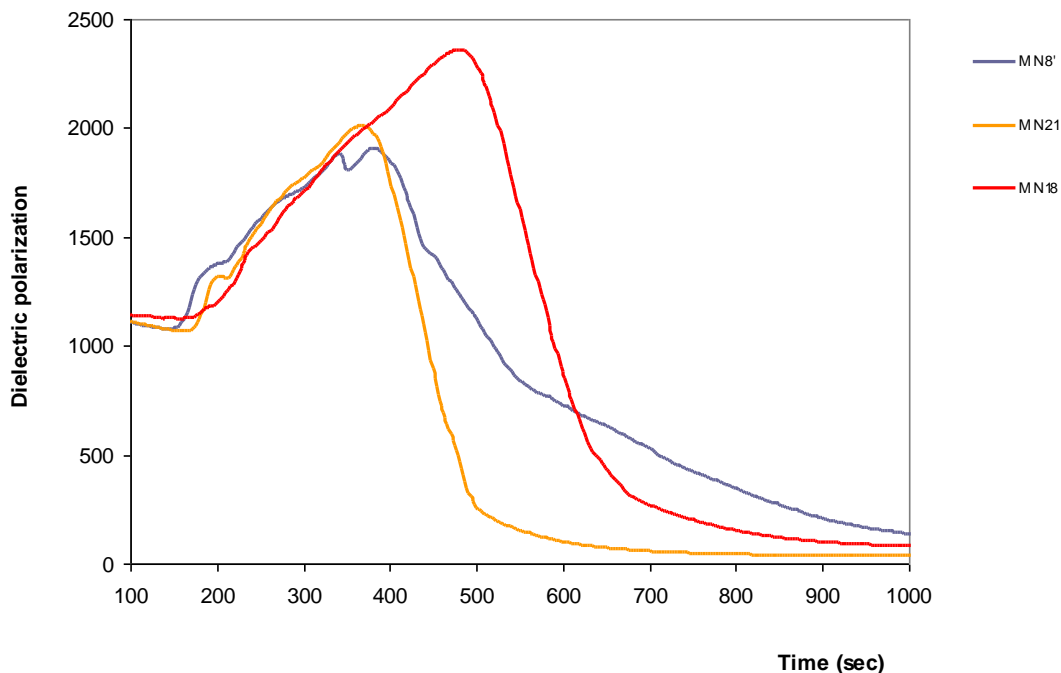


Fig. 3. Curves of variation of the dielectric polarization as a function of time during foaming for the MN8', MN21, and MN18 foams

Figure 3, which depicts the variation during foaming of the dielectric polarization values, in this respect a measure of cross-linking, provides a view of a rather different situation. It can be seen that the different surfactants retarded the cross-linking onset of the foams to a much different extent. That is, the addition of a surfactant had a major effect: it retarded the onset of cross-linking to a lesser or greater extent in relation to the maximum temperature represented in Fig. 2. This was rather different from the previously recorded behavior of formulations not containing a surfactant, in which cross-linking starts as the temperature of the reaction reaches its maximum (Basso *et al.* 2013). As seen in Fig. 3, the non-ionic surfactants retarded the onset of cross-linking to approximately 350 s for the MN8' and the MN21, that is, 150 s and 120 s later, respectively, than the time at which the maximum temperature was reached (Fig. 2). More interestingly, the non-ionic surfactant, which transforms under the acidic conditions used for these foams into a cationic surfactant, retarded the onset of cross-linking to an even greater degree (see MN18, Fig. 2). That is, for MN18, cross-linking started at 520 s, a whole 240 s later than the time corresponding to peak temperature. The question that should be asked is why such an effect occurred. Surfactants are known to produce a heat sink effect during the preparation of foam (Basso *et al.* 2013b), but that is not the case here, judging by the lack of depiction of any significant effect of this kind in Fig. 2. However, this effect can be explained because the PEG400 and surfactants present in MN8' and MN21 may act as plasticizers by increasing the intermolecular separation and thus decreasing molecular cross-linking (Marcilla and Beltran 2004). For MN18, the effect would be more severe due to the repulsions generated by the positive charge acquired under acid conditions.

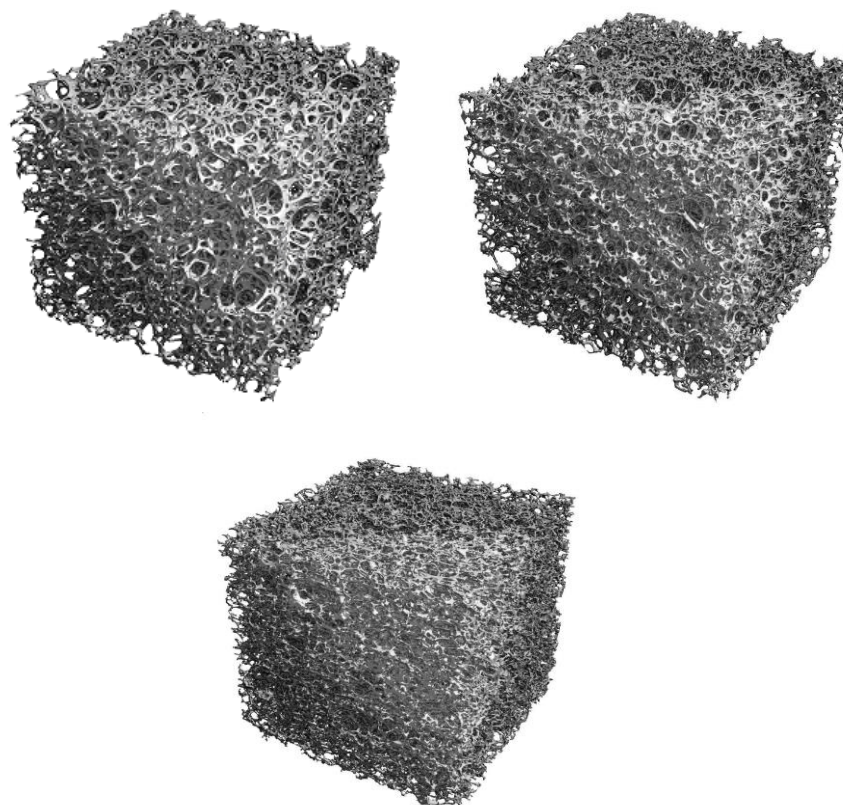


Fig. 4. Tomography of (a) MN18 foam, (b) MN21 foam, and (c) MN8' foam. Note the marked differences in structure and cells size among the three foams.

These three foams exhibited several marked structural and cells size differences during the tomography examination (Figs. 4 a, b, and c). In the absence of a surfactant, the ether is not well emulsified, and the same occurs for cationic emulsifications such as MN18, while it is well emulsified in MN8' and MN21. Therefore, these foams present a higher porosity development, in accordance with a further expansion as will be discussed below, having smaller cells size and thinner wall/struts than that for MN18. Then, the density of MN18 is higher.

The maximum temperature (Fig. 2) and pressure (Fig. 5) values occurred almost simultaneously, with the pressure maximum occurring slightly after the temperature maximum, by which time the rate of expansion had dropped to zero. A comparison of the different foams shows that the rate of foam expansion increased with increasing temperature, which was the outcome expected given that foaming depends exclusively on the evaporation of the solvent as a blowing agent.

Moreover, the pressure peak on the MN18 formulation was appreciably higher than the other 2 formulations as observed in Fig. 5. This could be due to insufficient stabilisation of the blowing agent and the higher density of MN18 foam.

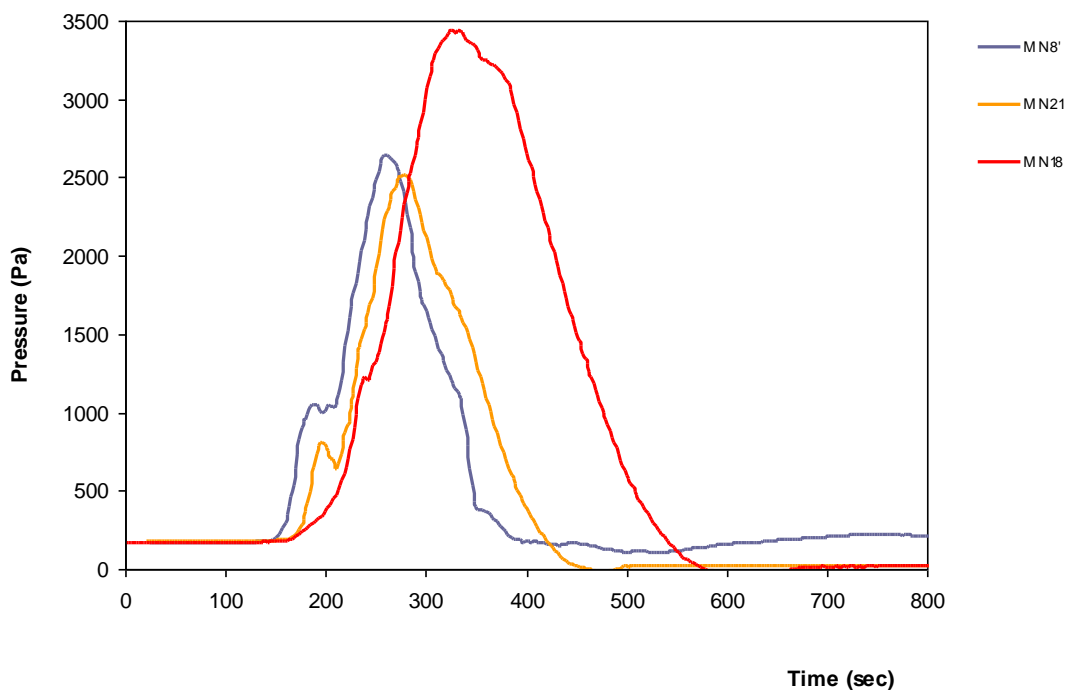


Fig. 5. Curves of foam pressure variation as a function of time during foaming for the MN8', MN21, and MN18 foams

The dielectric polarization value decreased as a function of time as a consequence of the progressive molecular immobilization due to cross-linking and hardening. The presence of a peak value of dielectric polarization could be attributed to two causes. First, the concomitant increase in temperature increased the molecular motion, resulting initially, before the cross-linking started, in an increase in the dielectric polarization value. Secondly, the presence of a dielectric polarization peak before the cross-linking began may indicate the presence of an intermediate competitive reaction. That is, water was being produced as a by-product during the polycondensation reaction. Therefore, a continuous increase in the number of charge carriers occurred initially during cross-

linking; consequently, the conductivity was increased instead of decreased by gelling/setting/curing. The presence of such an intermediate reaction is rather evident for MN8', MN21, and particularly for MN18, its occurrence with the third of which could be explained as a consequence of the cationic character under acidic conditions of the surfactant used.

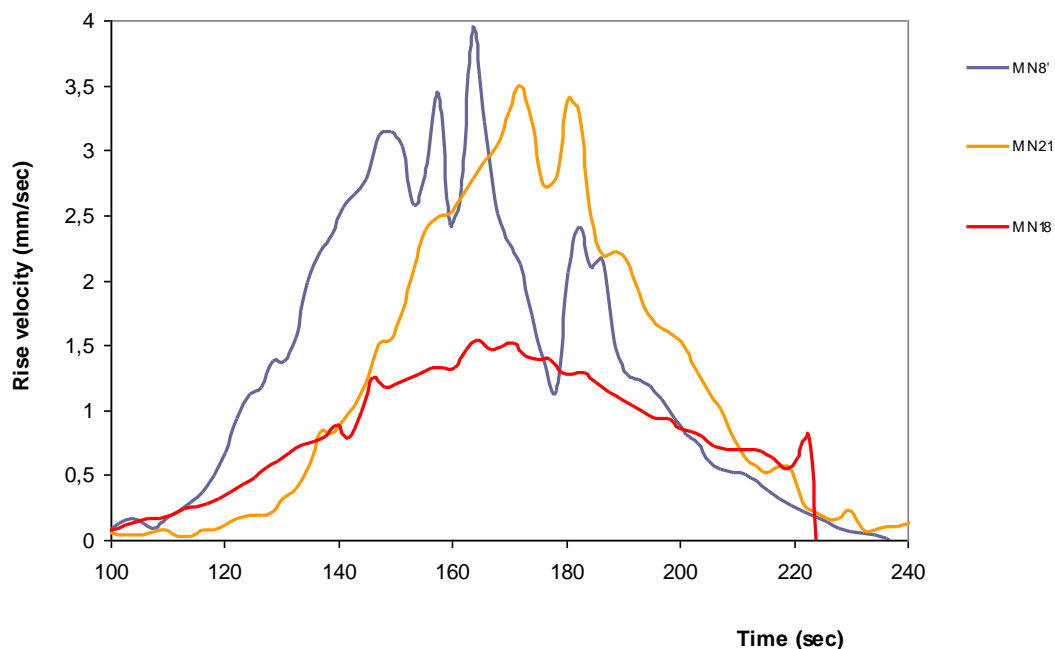


Fig. 6. Curves of the velocity of rising foam as a function of time during foaming of the MN8', MN21, and MN18 foams

In the case of the rate of expansion, the irregular shapes of the curves observed in Fig. 6 were due to the “free air rising” in the foam, as the temperature of the environment was not controlled. The rate of expansion is much more regular in a temperature-controlled environment. One further point of interest is that the slower rate of expansion of the MN18 foam contributed to its higher density in comparison to the two other foams, as seen in Table 1.

CONCLUSIONS

1. The use of a surfactant can markedly modify the dynamic behavior of tannin-based foams. The addition of a surfactant has a major effect on foam dynamics: it retards the onset of cross-linking to a lesser or greater extent in relation to the time at which the peak maximum temperature is reached.
2. Cationic surfactants, or non-ionic surfactants capable of transforming into cationic species under the acidic environmental conditions used for tannin-based foams, retard cross-linking more markedly than do non-ionic surfactants.

3. The maximum peaks of temperature and of internal foam pressure occur almost simultaneously, with the pressure maximum occurring slightly after the temperature maximum, by which time the rate of expansion has dropped to zero.

ACKNOWLEDGMENTS

The authors gratefully acknowledge the financial support of SILVA-INDUNOR. All the authors gratefully acknowledge the financial support of the CPER 2007-2013 “Structuration du Pole de Competitivite Fibres Grand Est” (Competitiveness Fibre Cluster), through local (Conseil General des Vosges), regional (Region Lorraine), national (DRRT and FNADT), and European (FEDER) funds.

REFERENCES CITED

- Basso, M. C., Giovando, S., Pizzi, A., Celzard, A., and Fierro, V. (2013a). “Tannin/furanic foams without blowing agents and formaldehyde,” *Ind. Crops & Prods.* 49, 17-22.
- Basso, M. C., Pizzi, A., and Celzard, A. (2013b). “Influence of formulation on the dynamics of preparation of tannin-based foams,” *Ind. Crops & Prods.* (in press).
- Celzard, A., Fierro, V., Amaral-Labat, G., Pizzi, A., and Torero, J. (2011). “Flammability assessment of tannin-based cellular materials,” *Polym. Deg. Stab.* 96(4), 477-482.
- Hildebrand, T., and Ruegsegger, P. (1996). “A new method for the model-independent assessment of thickness in three-dimensional images,” *J. Microsc.* 185, 57-75.
- Lacoste, C., Basso, M. C., Pizzi, A., Laborie, M.-P., and Celzard, A. (2013). “Pine tannin-based rigid foams: Mechanical and thermal properties,” *Ind. Crops & Prod.* 43, 245-250.
- Lacoste, C., Basso, M. C., Pizzi, A., Laborie, M.-P., Garcia, D., and Celzard, A. (2013b). “Bioresourced pine tannin/furanic foams with glyoxal and glutaraldehyde,” *Ind. Crops & Prod.* 45, 401-405.
- Li, X., Basso, M. C., Fierro, V., Pizzi, A., and Celzard, A. (2012a). “Chemical modification of tannin/furanic rigid foams by isocyanates and polyurethanes,” *Maderas Ciencia Technol.* 14(3), 257-265.
- Li, X., Essawy, H. A., Pizzi, A., Delmotte, L., Rode, K., Le Nouen, D., Fierro, V., and Celzard, A. (2012b). “Modification of tannin-based rigid foams using oligomers of a hyperbranched poly(amine-ester),” *J. Polym. Res.* 19(12), 1-9.
- Li, X., Pizzi, A., Cangemi, M., Fierro, V., and Celzard, A. (2012c). “Flexible natural tannin-based and protein-based biosourced foams,” *Ind. Crops & Prod.* 37(1), 389-393.
- Li, X., Srivastava, V. K., Celzard, A., and Leban, J. (2013b). “Nanotube reinforced tannin/furanic rigid foams,” *Ind. Crops & Prod.* 43, 636-639.
- Marcilla, A., and Beltran, M. (2004). “Mechanisms of plasticizers action,” *Handbook of Plasticizers*, Wypych George.
- Meikleham, N. E., and Pizzi, A. (1994). “Acid- and alkali-catalyzed tannin-based rigid foams,” *J. Appl. Polym. Sci.* 53(11), 1547-1556.
- Odgaard, A. (1997). “Three-dimensional methods for quantification of cancerous bone architecture,” *Bone* 20, 315-328.

- Odgaard, A., and Gundersen, H. J. (1993). "Quantification of connectivity in cancerous bone, with special emphasis on 3-D reconstructions," *Bone* 14, 173-182.
- Pasch, H., Pizzi, A., and Rode, K. (2001). "MALDI-TOF mass spectrometry of polyflavonoid tannins," *Polymer* 42(18), 7531-7539.
- Pizzi, A. (1983). *Wood Adhesives Chemistry and Technology*, Marcel Dekker, New York.
- Pizzi, A., Tondi, G., Pasch, H., and Celzard, A., (2008). "Maldi-ToF structure determination of complex thermoset network – Polyflavonoid tannin-furanic rigid foams," *J. Appl. Polym. Sci.* 110(3), 1451-1456.
- Sernek, M., and Kamke, F. E. (2007). "Application of dielectric analysis for monitoring the cure process of phenol formaldehyde adhesive," *Int. J. Adhesion Adhes.* 27(7), 562-567.
- Tadros, T. F. (2005). *Applied Surfactants: Principles and Applications*, Xiley-VCH Verlag GmbH & Co. KGaA, Weinheim.
- Tondi, G., and Pizzi, A. (2009). "Tannin based rigid foams: Characterisation and modification," *Ind. Crops & Prod.* 29(2-3), 356-363.
- Tondi, G., Oo, C. W., Pizzi, A., Trosa, A., and Thevenon, M.-F. (2009a). "Metal adsorption of tannin-based rigid foams," *Ind. Crops & Prod.* 29(2-3), 336-340.
- Tondi, G., Pizzi, A., and Olives, R. (2008). "Natural tannin-based rigid foams as insulation in wood construction," *Maderas Ciencia Tecnol.* 10(3), 219-227.
- Tondi, G., Zhao, W., Pizzi, A., Du, G., Fierro, V., and Celzard, A. (2009b). "Tannin-based rigid foams: A survey of chemical and physical properties," *Bioresour. Technol.* 100(21), 5162-5169.

Article submitted: July 12, 2013; Peer review completed: August 6, 2013; Revised version received and accepted: September 12, 2013; Published: September 26, 2013.